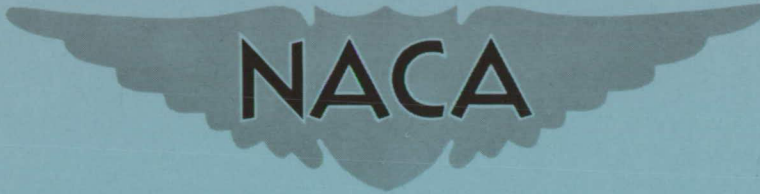


CONFIDENTIAL

Copy 321  
RM H55E20a



# RESEARCH MEMORANDUM

FLIGHT MEASUREMENTS OF HORIZONTAL-TAIL  
LOADS ON THE BELL X-5 RESEARCH AIRPLANE AT A  
SWEEP ANGLE OF 58.7°

By Robert D. Reed

High-Speed Flight Station  
Edwards, Calif.

CLASSIFICATION CHANGED TO UNCLASSIFIED  
AUTHORITY: NACA RESEARCH ABSTRACT NO. 97  
DATE: FEBRUARY 24, 1956

WHL

CLASSIFIED DOCUMENT

Declassified

...ing the National Defense of the United States within the meaning  
secs. 793 and 794, the transmission or revelation of which in any  
manner to an unauthorized person is prohibited by law.

NATIONAL ADVISORY COMMITTEE  
FOR AERONAUTICS

WASHINGTON

July 21, 1955

CONFIDENTIAL

## NATIONAL ADVISORY COMMITTEE FOR AERONAUTICS

## RESEARCH MEMORANDUM

FLIGHT MEASUREMENTS OF HORIZONTAL-TAIL  
LOADS ON THE BELL X-5 RESEARCH AIRPLANE AT A  
SWEEP ANGLE OF  $58.7^\circ$ 

By Robert D. Reed

## SUMMARY

A flight investigation was made at altitudes of 40,000, 25,000 and 15,000 feet to determine the horizontal-tail loads of the Bell X-5 research airplane at a sweep angle of  $58.7^\circ$  over the lift range of the airplane for Mach numbers from 0.61 to 1.00. The horizontal-tail loads were found to be nonlinear with lift throughout the lift ranges tested at all Mach numbers except at a Mach number of 1.00. The balancing tail loads reflected the changes which occur in the wing characteristics with increasing angle of attack. The nonlinearities were, in general, more pronounced at the higher angles of attack near the pitch-up where the balancing tail loads indicate that the wing-fuselage combination becomes unstable.

No apparent effects of altitude on the balancing tail loads were evident over the comparable lift ranges of these tests at altitudes from 40,000 feet to 15,000 feet.

Comparisons of balancing tail loads obtained from flight and wind-tunnel tests indicated discrepancies in absolute magnitudes, but the general trends of the data agree. Some differences in absolute magnitude may be accounted for by the tail load carried inboard of the strain-gage station and the load induced on the fuselage by the presence of the tail. These loads were not measured in flight.

## INTRODUCTION

As part of the cooperative Air Force—Navy—NACA transonic flight research program, the National Advisory Committee for Aeronautics is utilizing the Bell X-5 variable-sweep research airplane for flight investigations at the NACA High-Speed Flight Station at Edwards, Calif. The

primary purpose of these flight investigations is to determine the loads, stability and control characteristics, lift and drag, and buffeting characteristics of the airplane at selected sweep angles. Because of the interest in the loads and stability characteristics at high sweep angles, the first complete investigation on this airplane was made at a wing sweep angle of  $58.7^\circ$ , the maximum sweep angle obtainable. Preliminary results of horizontal tail-load measurements at various sweep angles during demonstration tests are presented in reference 1. Results of the complete tail loads investigation at a wing sweep angle of  $58.7^\circ$  are given in this paper.

## SYMBOLS

b	wing span, ft
$C_{N_A}$	airplane normal-force coefficient, $nW/qS$
$C_{N_t}$	tail normal-force coefficient, $L_t/qS_t$
$C_{N_t}^{Bal}$	tail normal-force coefficient required to balance wing-fuselage pitching-moment coefficient, $L_{t}^{Bal}/qS_t$
c	chord at any section along span, ft
g	acceleration due to gravity, $ft/sec^2$
$h_p$	pressure altitude, ft
$i_t$	stabilizer setting referred to airplane longitudinal axis, (positive when leading edge of stabilizer is up), deg
$L_t$	measured aerodynamic horizontal-tail load, (up load positive), lb
$L_{t}^{Bal}$	tail normal force required to balance wing-fuselage pitching moment, lb

M	Mach number
n	airplane normal acceleration, g units
q	dynamic pressure, $\frac{1}{2}\rho V^2$ , lb/sq ft
S	area of wing bounded by leading edge and trailing edge extended to airplane line of symmetry disregarding fillets, $2 \int_0^{b/2} c \, dy$ , sq ft
$S_t$	area of horizontal tail, sq ft
V	free-stream velocity, ft/sec
W	airplane gross weight, lb
y	lateral distance, ft
$\alpha_i$	indicated airplane angle of attack, deg
$\delta_e$	elevator position, deg
$\dot{\theta}$	pitching velocity, (positive nose up), radians/sec
$\ddot{\theta}$	pitching angular acceleration, radians/sec <sup>2</sup>
$\rho$	mass density of air, slugs/cu ft

## AIRPLANE

The Bell X-5 research airplane incorporates a wing which is variable in flight between sweep angles of about 20° and about 58.7°. A photograph of the airplane in the 58.7° sweep configuration utilized in this investigation is shown in figure 1. A three-view drawing of the airplane is presented in figure 2. The airplane physical characteristics in the 58.7° sweptback configuration are given in table I.

## INSTRUMENTATION AND ACCURACY

Standard NACA recording instruments were installed in the Bell X-5 research airplane to measure the following quantities pertinent to this investigation:

- Airspeed
- Altitude
- Angle of attack and angle of sideslip
- Normal, longitudinal, and transverse accelerations
- Pitching angular velocity and acceleration
- Rolling angular velocity
- Yawing angular velocity and acceleration
- Control positions
- Wing sweep angle

Shear and bending moments on the horizontal tail panel were measured by means of strain gages installed on the spar and skin at the root station 14.5 inches from the airplane center line as shown in figure 3. The outputs of these strain gages were recorded on a multi-channel recording oscillograph. The data presented have been corrected for the inertia of the tail and are therefore the aerodynamic loads acting on the tail. Based on the results of a static calibration and an evaluation of the strain-gage responses in flight, the estimated accuracy of the measured horizontal-tail loads is  $\pm 75$  pounds. This accuracy results in a maximum estimated error in tail normal-force coefficient of  $\pm 0.02$  for the lowest dynamic pressure encountered.

In order to minimize the errors in total pressure measurement, an NACA type A-6 total pressure head (ref. 2) was mounted on the nose boom and the static pressure error was determined in flight. The total estimated error in Mach number is within  $\pm 0.01$ . The maximum error in the determination of the airplane normal-force coefficient is  $\pm 0.03$ . The angle of attack was measured by a vane located on the nose boom and is presented in this paper as measured data.

## TESTS

The tests were conducted in the clean configuration with the slats closed and consisted of symmetrical maneuvers performed primarily by using the elevator control at altitudes of 40,000, 25,000, and 15,000 feet. The Mach number range was from  $M \approx 0.61$  to  $M \approx 1.00$  at 40,000 feet,  $M \approx 0.61$  to  $M \approx 0.96$  at 25,000 feet, and  $M \approx 0.61$  to  $M \approx 0.90$  at 15,000 feet. The maneuvers at 40,000 feet covered the available lift range of the airplane. Only moderate lifts were reached at 25,000 feet

and 15,000 feet, however, to avoid pitch-up at the lower altitudes. Reynolds number (based on the wing mean aerodynamic chord) at 40,000 feet varied from  $11.5 \times 10^6$  to  $19.0 \times 10^6$  and at 15,000 feet varied from  $38.0 \times 10^6$  to  $43.0 \times 10^6$ . The airplane center of gravity remained near 45 percent mean aerodynamic chord throughout the tests.

## RESULTS AND DISCUSSION

Data obtained during representative maneuvers performed at 40,000 feet over the Mach number range of 0.61 to 1.00 are presented in figure 4 as variations with angle of attack. The elevator control was used for all maneuvers shown except at  $M \approx 1.00$  where high stick forces required use of the power-operated stabilizer control. The measured aerodynamic tail loads are generally nonlinear throughout the angle-of-attack and Mach number range except at  $M \approx 1.00$  where the tail load variation with angle of attack is essentially linear. For the maneuvers between  $M \approx 0.61$  and  $M \approx 0.96$  rapid increases in the pitching velocity and acceleration occur at the higher angles of attack accompanied by a reversal of the slope of the measured aerodynamic tail load.

The balancing tail loads were obtained by correcting the measured aerodynamic tail loads of figure 4 to a condition of zero thrust and zero pitching acceleration (ref. 3) and are shown in figure 5 as a variation with airplane normal-force coefficient. The balancing tail loads determined from maneuvers at altitudes of 25,000 feet and 15,000 feet are also shown in figure 5. The differences in the balancing tail loads obtained at the three altitudes over comparable lift ranges are small and are generally within the accuracy of the measurements. These results indicate there are no apparent effects of altitude on the tail loads. Therefore, subsequent presentation and discussion will be concerned only with data obtained at 40,000 feet, the altitude at which it is possible to describe the tail load characteristics over the complete lift range of the airplane.

The curves of figure 5 show generally nonlinear characteristics throughout the lift ranges investigated at any Mach number to 0.96. At  $M \approx 1.00$  the curve appears to be linear, however the lift range investigated at  $M \approx 1.00$  was considerably lower than the lift range covered at the lower Mach numbers. At all Mach numbers below 1.00 the trends of the curves are similar and may be broken into three separate lift ranges. The three lift regions are indicated on the curves in figure 5 by the two vertical lines above the curves. In general the tail loads remain constant or show a slight positive increase with lift in the low lift region ( $C_{NA} = 0$  to the first vertical line), increase negatively

in the second lift region (lift region between the two vertical lines), and increase positively in the highest lift region. These trends indicate slightly negative to neutral wing-fuselage stability in the low lift region, positive wing-fuselage stability in the moderate lift region, and an unstable wing-fuselage in the high lift region.

The wing characteristics (ref. 4) also indicated distinct changes for the same general three lift ranges. The wing pitching moments indicated a rearward wing center-of-pressure movement from the low to moderate lift region followed by a forward movement as the high lift region was entered. The wing center-of-pressure movements in the three lift regions are reflected in the trends of the balancing tail loads, indicating that the wing is contributing to these trends. The vertical line separating the moderate and high lift region also approximately coincides with the reduction in airplane longitudinal stability as defined by the variation of elevator or stabilizer angle with angle of attack (ref. 5).

Figure 6 shows a comparison of the variation of balancing tail normal-force coefficient with airplane normal-force coefficient as obtained from flight and wind-tunnel tests. The wind-tunnel data were obtained by correcting the wind-tunnel tail-off pitching-moment data of reference 6 to the flight center-of-gravity position and by converting the data to balancing tail normal-force coefficient. The general trends of the flight and wind-tunnel results agree, but discrepancies in absolute level are apparent. A part of this difference may be due to the fact that only the tail loads outboard of the strain-gage station were measured, and that the lift of the exposed tail area inboard of the strain gages and the induced lift on the fuselage due to the presence of the tail were not measured.

To illustrate the effects of Mach number on the balancing tail loads, figure 7 shows the variations of tail normal-force coefficient with Mach number at several constant airplane normal-force coefficients up to  $C_{N_A} = 0.4$ . Above a normal-force coefficient of 0.4 for the higher Mach numbers in the lift region above the pitch-up no consistent Mach number effects could be separated from the lift effects. The curves indicate no changes in the balancing tail loads with increasing Mach number to  $M = 0.9$ , but show a negative increase thereafter for airplane normal-force coefficients above  $C_{N_A} = 0$ .

#### CONCLUDING REMARKS

An investigation of the horizontal-tail loads on the Bell X-5 research airplane at a sweep angle of  $58.7^\circ$  has indicated that the horizontal-tail loads are nonlinear with lift throughout the lift ranges

tested at all Mach numbers except at a Mach number of approximately 1.00. The balancing tail loads reflected changes which occur in the wing characteristics with increasing angle of attack. The nonlinearities of the horizontal-tail loads were generally more pronounced at the higher angles of attack near the pitch-up where the balancing tail loads indicate that the wing-fuselage combination becomes unstable.

No apparent effects of altitude on the balancing tail loads were evident over the comparable lift ranges of these tests at altitudes from 40,000 feet to 15,000 feet.

Comparisons of balancing tail loads obtained from flight and wind-tunnel tests indicated discrepancies in absolute magnitudes, but the general trends of the data agree. Some differences in absolute magnitude may be accounted for by the tail load carried inboard of the strain-gage station and the load induced on the fuselage by the presence of the tail. These loads were not measured in flight.

High-Speed Flight Station,  
National Advisory Committee for Aeronautics,  
Edwards, Calif., May 3, 1955.

## REFERENCES

1. Rogers, John T., and Dunn, Angel H.: Preliminary Results of Horizontal-Tail Load Measurements of the Bell X-5 Research Airplane. NACA RM L52G14, 1952.
2. Gracey, William, Letko, William, and Russell, Walter R.: Wind-Tunnel Investigation of a Number of Total-Pressure Tubes at High Angles of Attack - Subsonic Speeds. NACA TN 2331, 1951. (Supersedes NACA RM L50G19.)
3. Rogers, John T.: Horizontal-Tail Load Measurements at Transonic Speeds of the Bell X-1 Research Airplane. NACA RM L53F30, 1953.
4. Banner, Richard D., Reed, Robert D., and Marcy, William L.: Wing-Load Measurements of the Bell X-5 Research Airplane at a Sweep Angle of 58.7°. NACA RM H55A11, 1955.
5. Finch, Thomas W., and Walker, Joseph A.: Flight Determination of the Static Longitudinal Stability Boundaries of the Bell X-5 Research Airplane With 59° Sweepback. NACA RM L53A09b, 1953.
6. Bielat, Ralph P., and Campbell, George S.: A Transonic Wind-Tunnel Investigation of the Longitudinal Stability and Control Characteristics of a 0.09-Scale Model of the Bell X-5 Research Airplane and Comparison With Flight. NACA RM L53H18, 1953.

TABLE I  
 PHYSICAL CHARACTERISTICS OF BELL X-5 RESEARCH AIRPLANE  
 AT A SWEEP ANGLE OF 58.7°

Airplane:

Weight, lb:	
Full fuel . . . . .	10,006
Less fuel . . . . .	7,894
Center-of-gravity position, percent M.A.C.:	
Full fuel . . . . .	45.0
Less fuel . . . . .	45.5
Moments of inertia for 58.7° sweep (clean configuration full fuel), slug-ft <sup>2</sup> :	
About X-axis . . . . .	5,165
About Y-axis . . . . .	9,495
About Z-axis . . . . .	10,110
Tail length, distance from 0.25 M.A.C. of horizontal tail to airplane center of gravity (0.45 M.A.C. of wing), ft . . . . .	16.75

Wing:

Airfoil section (perpendicular to 38.02-percent-chord line):	
Root . . . . .	NACA 64 (10) A011
Tip . . . . .	NACA 64 (08) A008.28
Sweep angle at 0.25 chord, deg . . . . .	58.7
Area, sq ft . . . . .	183.7
Span, ft . . . . .	20.1
Span between equivalent tips, ft . . . . .	19.3
Aspect ratio . . . . .	2.20
Taper ratio . . . . .	0.411
Mean aerodynamic chord, ft . . . . .	9.95
Location of leading edge of M.A.C., fuselage station . . . . .	101.2
Incidence root chord, deg . . . . .	0
Dihedral, deg . . . . .	0
Geometric twist, deg . . . . .	0

Horizontal tail:

Airfoil section (parallel to fuselage center line) . . . . .	NACA 65A006
Area, sq ft . . . . .	31.5
Span, ft . . . . .	9.56
Aspect ratio . . . . .	2.9
Taper ratio . . . . .	0.371
Sweep angle at 0.25-percent chord, deg . . . . .	45
Mean aerodynamic chord, ft . . . . .	3.57
Position of 0.25 M.A.C., fuselage station . . . . .	355.6
Stabilizer travel, (power actuated), deg:	
Leading edge up . . . . .	4.5
Leading edge down . . . . .	7.5
Elevator (20.8 percent overhang balance, 31.5 percent span):	
Area rearward of hinge line, sq ft . . . . .	6.9
Travel from stabilizer, deg:	
Up . . . . .	25
Down . . . . .	20
Chord, percent horizontal tail chord . . . . .	30
Moment area rearward of hinge line (total), in. <sup>3</sup> . . . . .	4,200

Vertical tail:

Airfoil section (parallel to rear fuselage center line) . . . . .	NACA 65A006
Area, (above rear fuselage center line), sq ft . . . . .	25.8
Span, perpendicular to rear fuselage center line, ft . . . . .	6.17
Aspect ratio . . . . .	1.47
Sweep angle of leading edge, deg . . . . .	46.6



Figure 1.- Photograph of the X-5 research airplane. L-87574

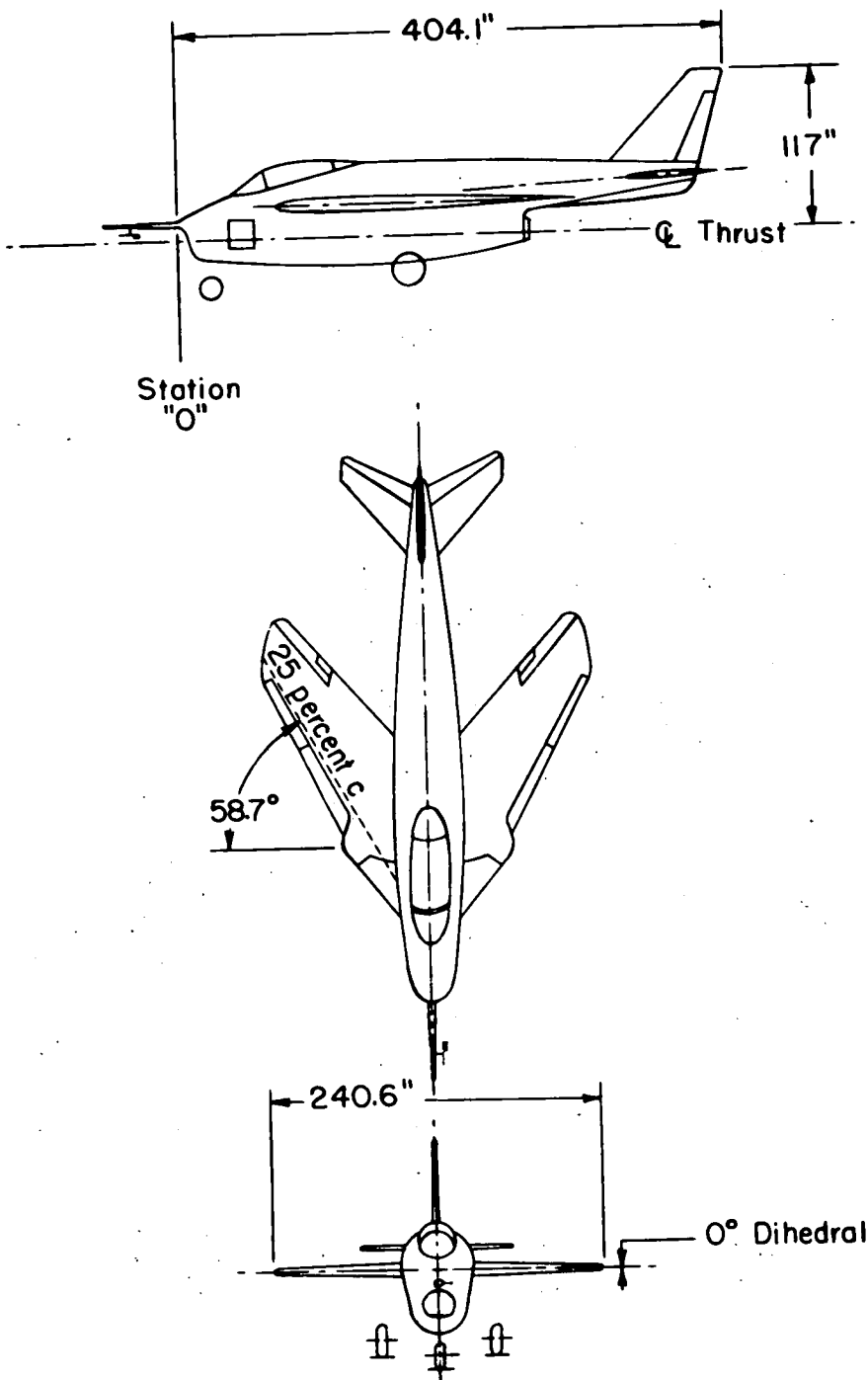


Figure 2.- Three-view drawing of the Bell X-5 research airplane at 58.7° sweepback.

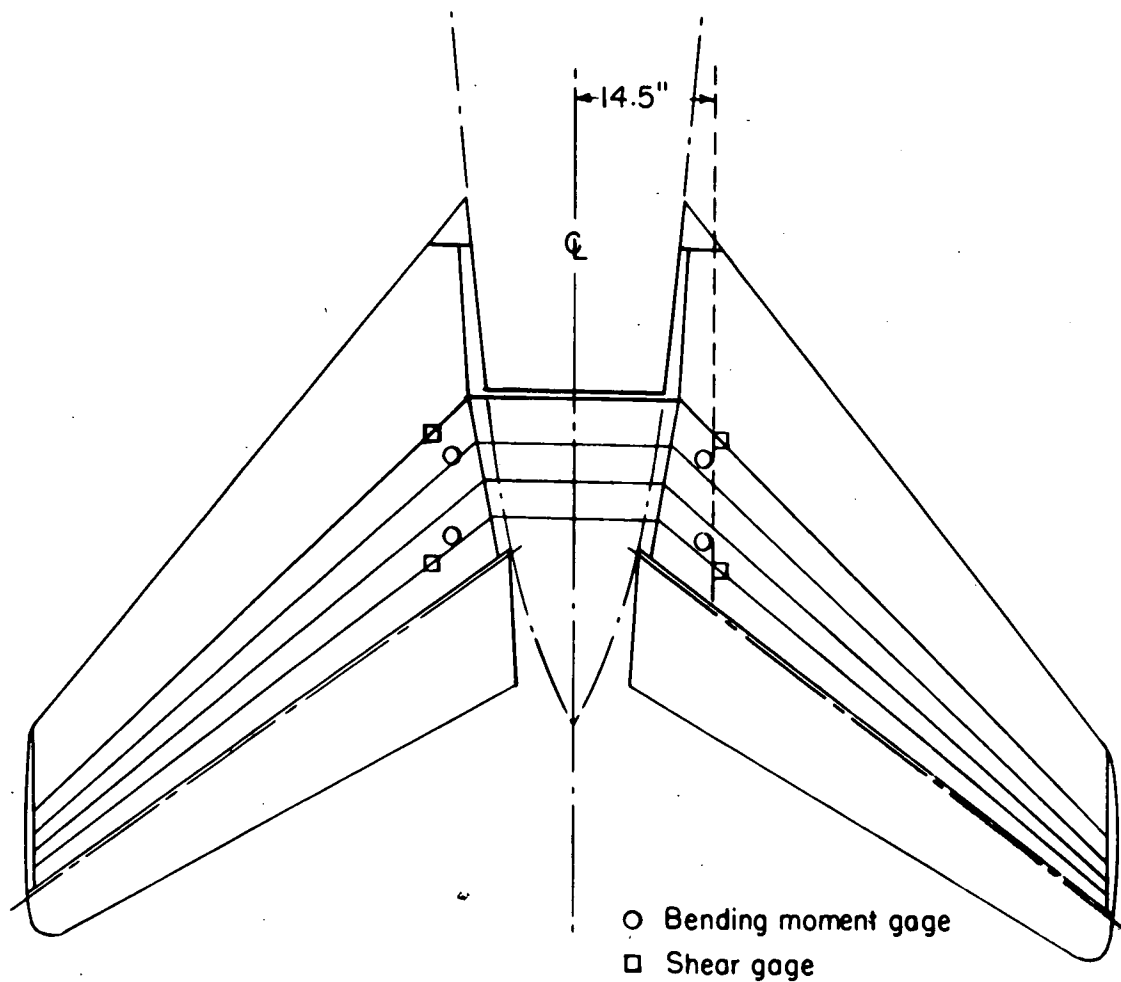
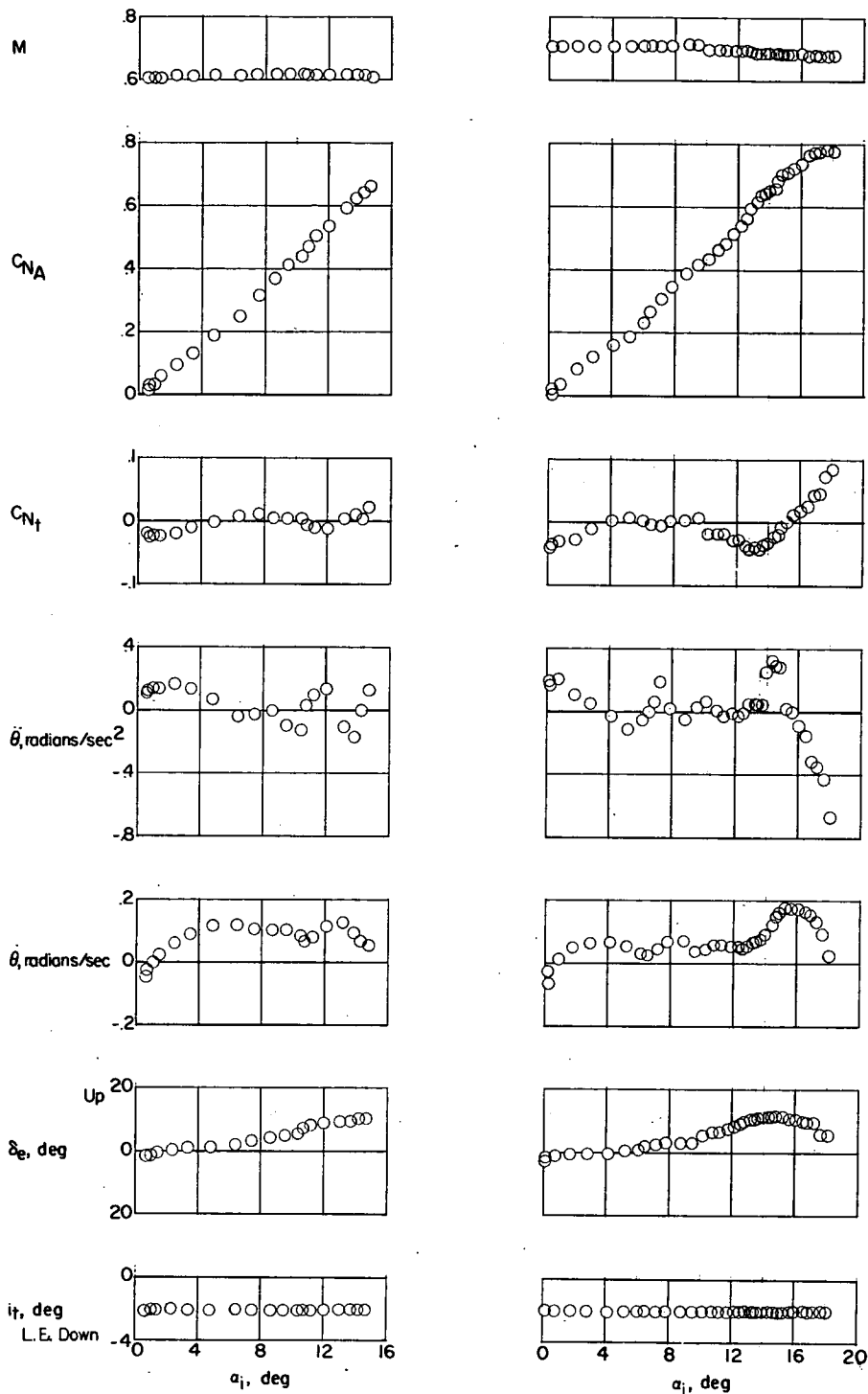


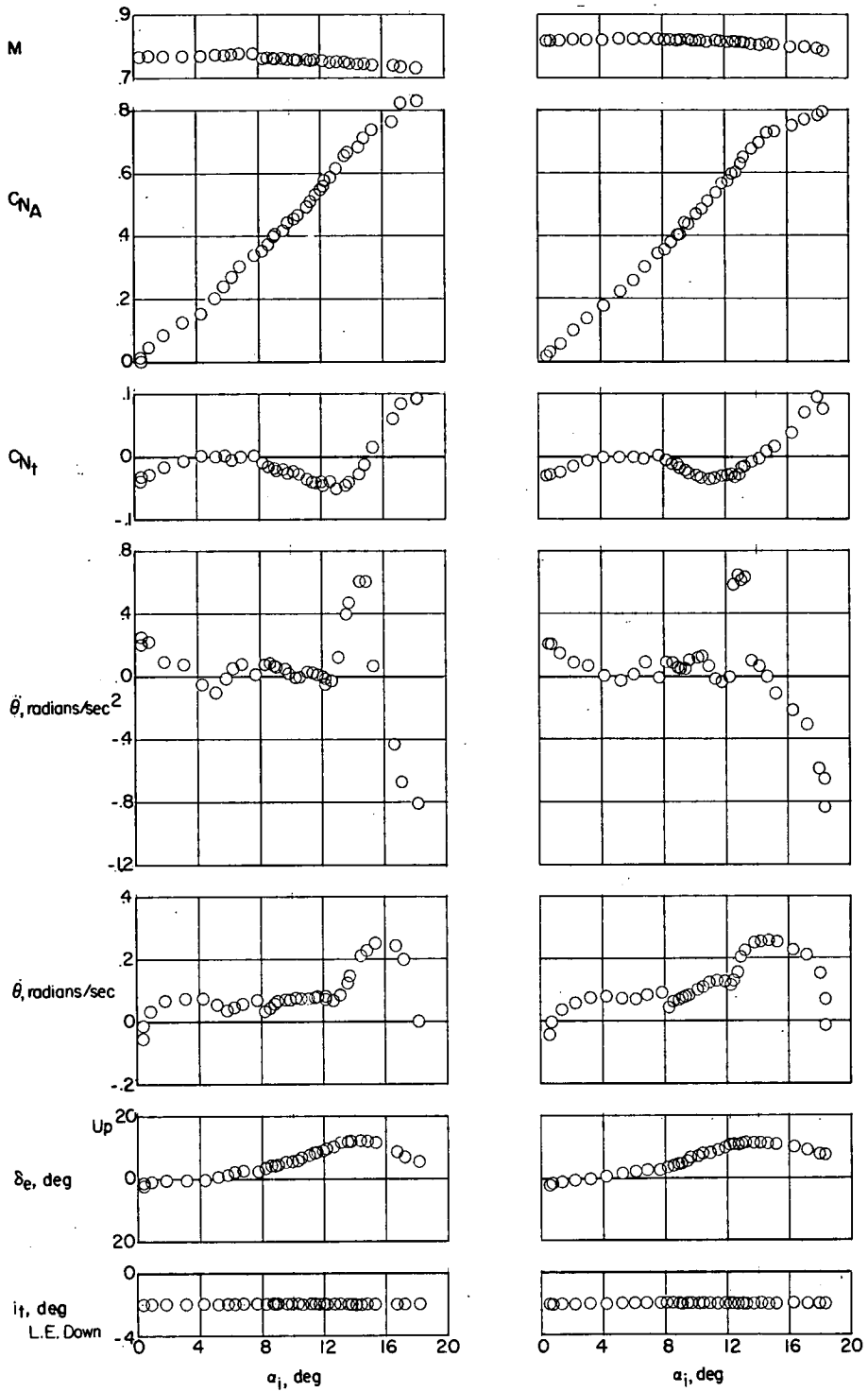
Figure 3.- Horizontal tail of X-5 airplane showing the location of the strain gages.



(a)  $M \approx 0.61$ .

(b)  $M \approx 0.70$ .

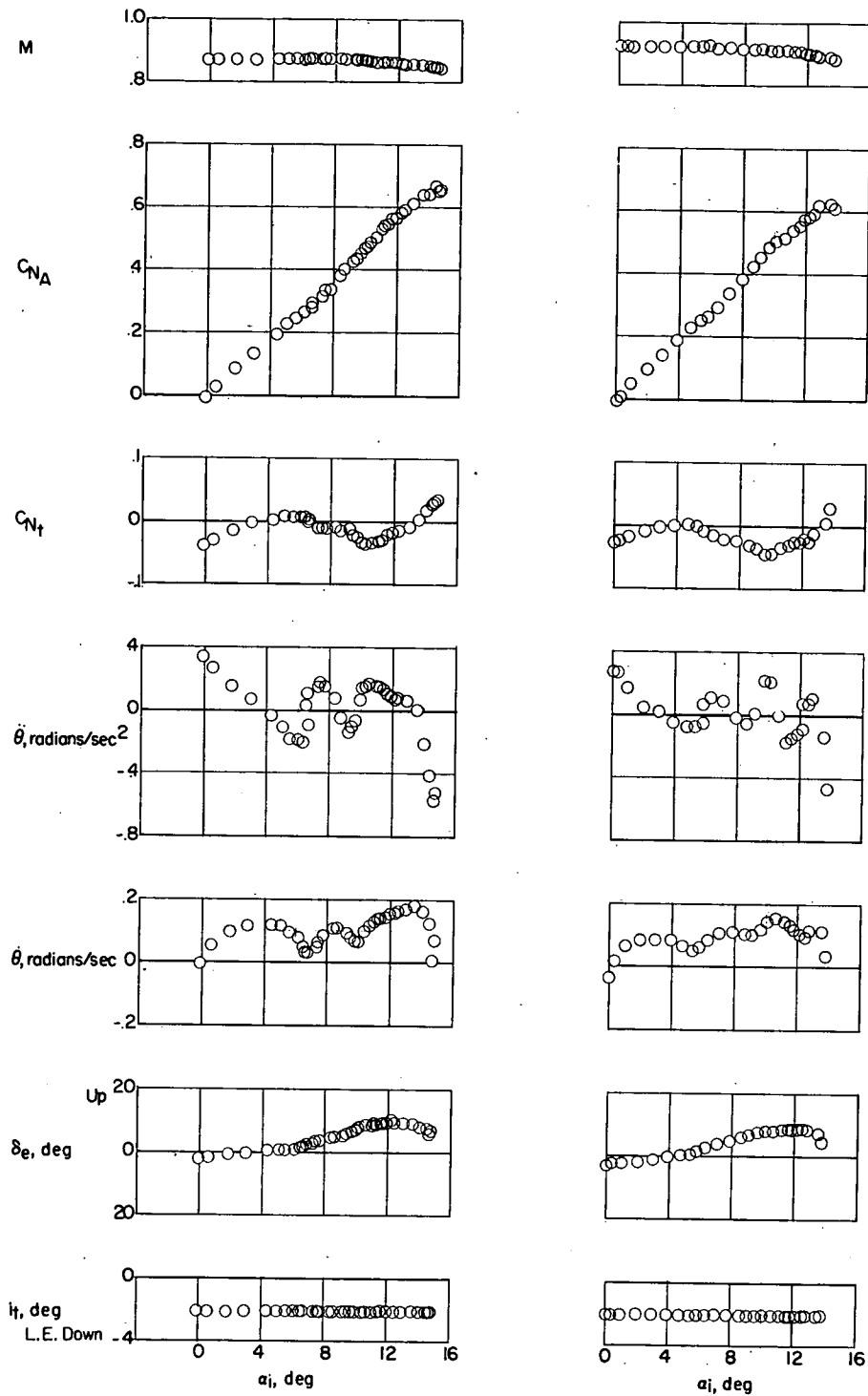
Figure 4.- Variations of measured quantities with angle of attack for representative maneuvers over the Mach number range from 0.61 to 1.00.



(c)  $M \approx 0.76$ .

(d)  $M \approx 0.81$ .

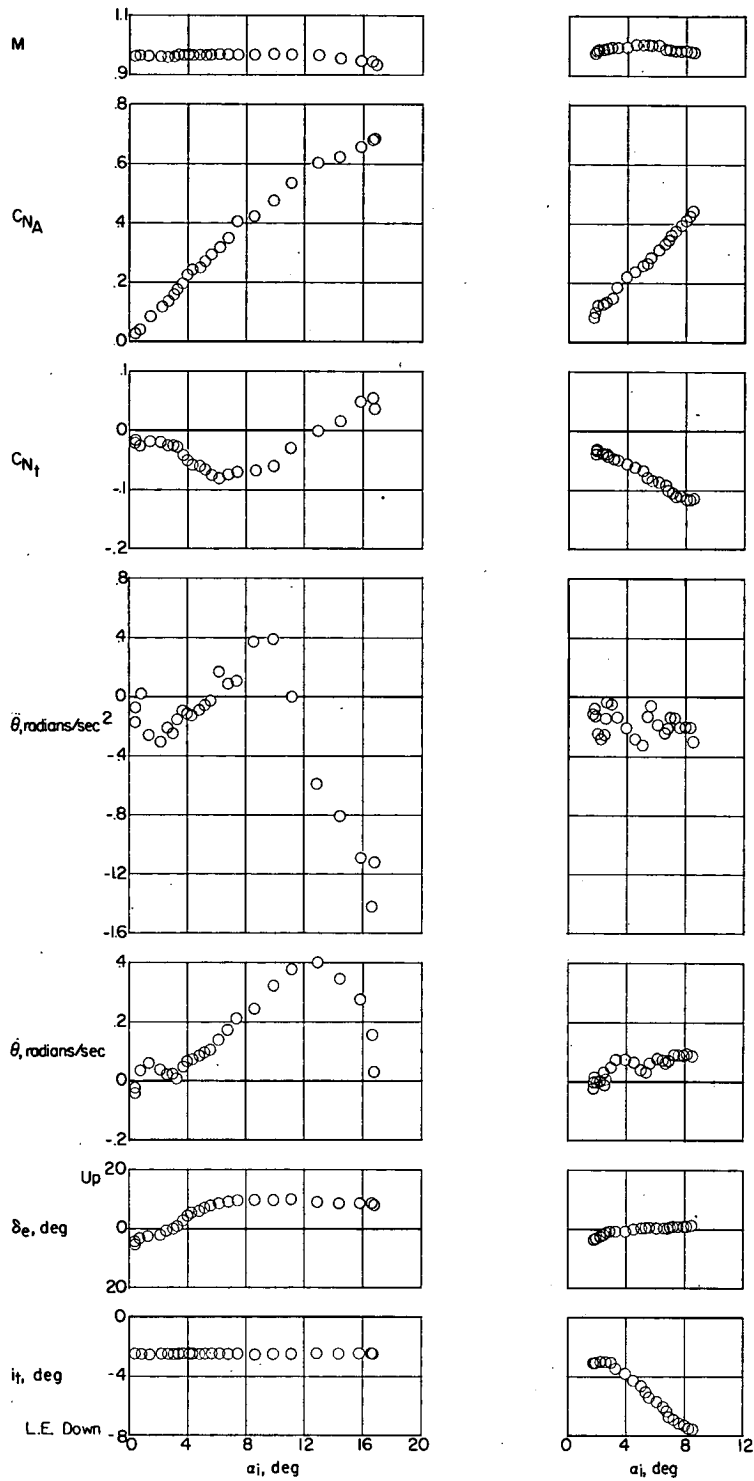
Figure 4.- Continued.



(e)  $M \approx 0.86$ .

(f)  $M \approx 0.90$ .

Figure 4.- Continued.



(g)  $M \approx 0.96$ .

(h)  $M \approx 1.00$ .

Figure 4.- Concluded.

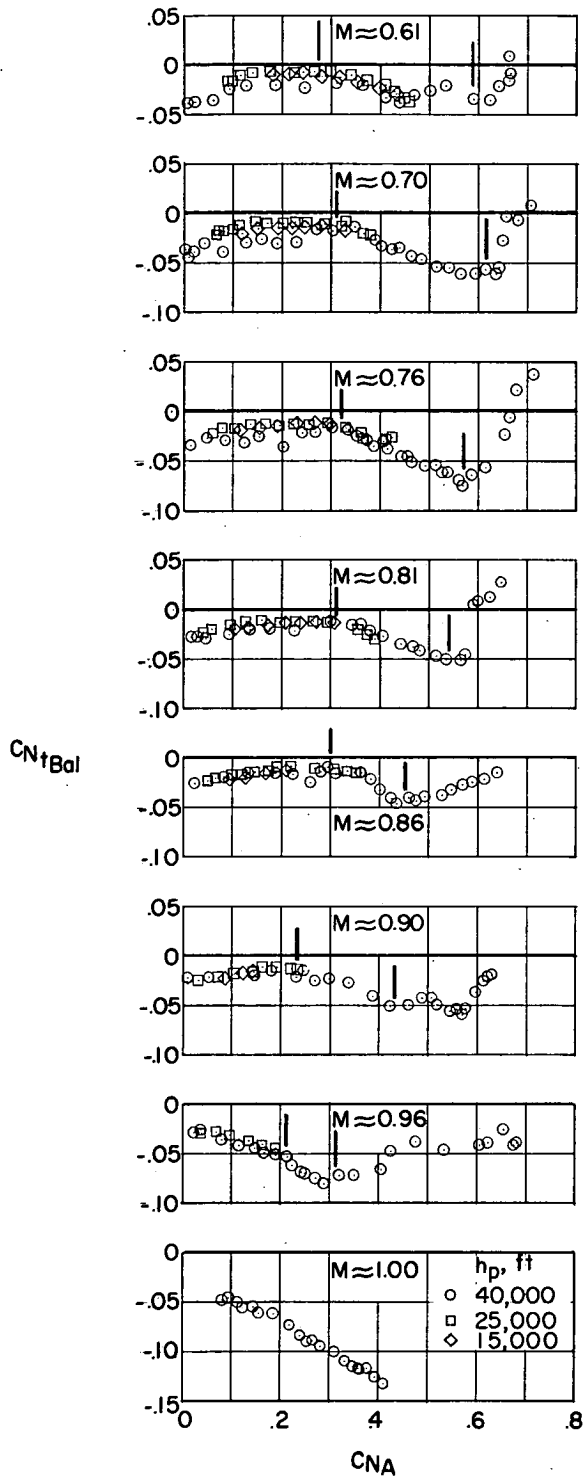


Figure 5.- Variation of balancing tail normal-force coefficient with airplane normal-force coefficient for representative maneuvers over the Mach number range from 0.61 to 1.00.

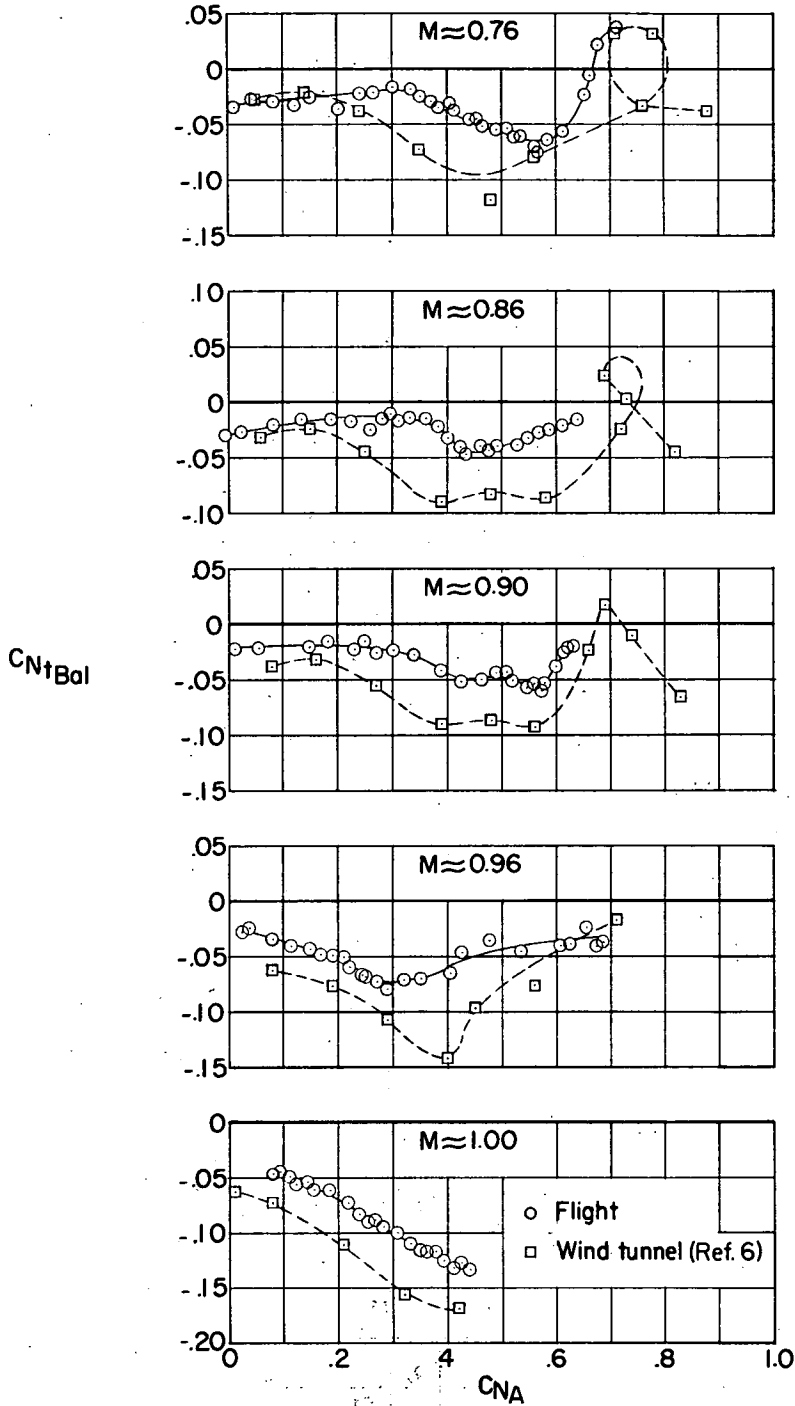


Figure 6.- Variation of balancing tail normal-force coefficient with airplane normal-force coefficient for representative maneuvers over the Mach number range from 0.76 to 1.00. The wind-tunnel data shown are corrected to the airplane center of gravity at 45 percent mean aerodynamic chord.

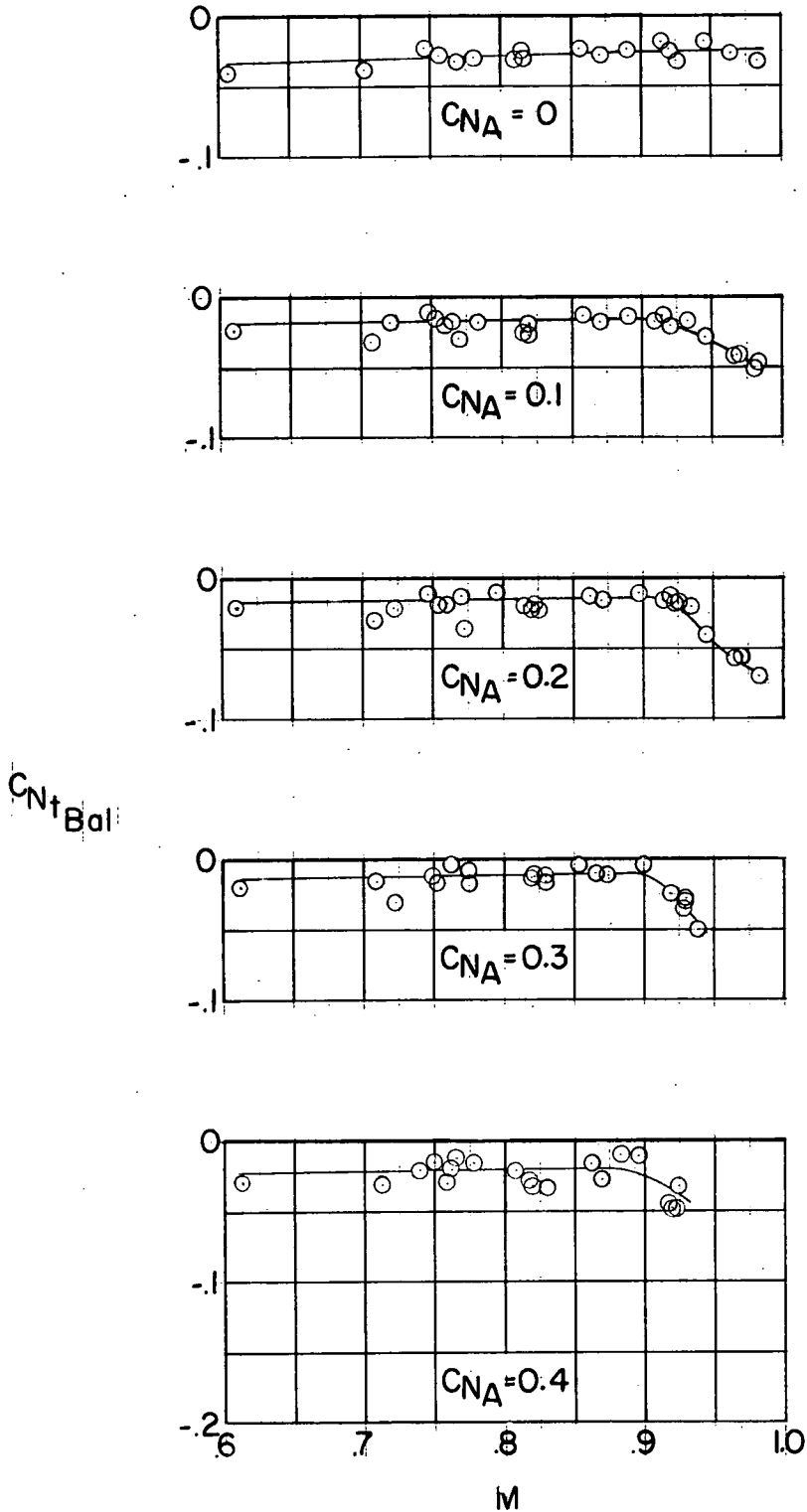


Figure 7.- Variation of balancing tail normal-force coefficient with Mach number for constant values of airplane normal-force coefficient.